Practical Multi-Cluster Consensus for Euler-Lagrangian Systems with Unknown Parameters using Prescribed Performance Control

Gopika R[1], Shubham Sawarkar[2], V. Resmi[3], Rakesh R. Warier[4], Pushpak Jagtap[2], and Sarang Dhongdi C[1]

[1]Birla Institute of Technology & Science Pilani - K K Birla Goa Campus
[2]Indian Institute of Science Robert Bosch Centre for Cyber-Physical Systems
[3]PTM Govt College Perinthalmanna
[4]National Institute of Technology Calicut Department of Electrical Engineering

November 25, 2024

Abstract

The paper addresses the challenge of achieving practical multi-cluster consensus among agents interacting through a matrix-weighted graph. The objective is to coordinate the agents to effectively capture or escort a moving target. Each agent satisfies Euler-Lagrange (EL) dynamics, whose parameters may be unknown, and is subject to external disturbances. We propose a multi-cluster control framework that ensures all agents within a cluster converge to a common trajectory, while individual clusters maintain a specific formation around the moving target. A prescribed performance control scheme is developed to guarantee that relative state trajectories remain within user-defined performance bounds throughout the task. The closed loop system under the proposed control scheme is analytically proven to achieve practical multi-cluster consensus and satisfaction of user-defined performance bounds without requiring knowledge of system parameters. The proposed framework supports various consensus scenarios, including consensus, bipartite consensus, and multi-cluster consensus, offering flexibility in adjusting both the number of clusters and the number of agents in each cluster. We provide numerical simulations to validate the theoretical results.

Practical Multi-Cluster Consensus for Euler-Lagrangian Systems with Unknown Parameters using Prescribed Performance Control

Gopika R[1] | **Shubham Sawarkar[2]** | **V. Resmi[3,4]** | **Rakesh R. Warier[5]** | **Pushpak Jagtap[2]** | **Sarang C Dhongdi[1]**

[1]Department of Electrical, Electronics and Instrumentation Engineering, BITS Pilani, K K Birla Goa Campus, Goa, India

[2]Center for Cyber-Physical Systems and Department of Aerospace Engineering, Indian Institute of Science, Bangalore, India

[3]Department of Physics, PTM Govt. College Perinthalmanna, Kerala, India

[4]Department of Physics, Govt. Victoria College, Palakkad, Kerala, India

[5]Department of Electrical Engineering, National Institute of Technology Calicut, Kerala, India

Correspondence

Corresponding author: Gopika R
Email: p20190058@goa.bits-pilani.ac.in

Abstract

The paper addresses the challenge of achieving practical multi-cluster consensus among agents interacting through a matrix-weighted graph. The objective is to coordinate the agents to effectively capture or escort a moving target. Each agent satisfies Euler-Lagrange (EL) dynamics, whose parameters may be unknown, and is subject to external disturbances. We propose a multi-cluster control framework that ensures all agents within a cluster converge to a common trajectory, while individual clusters maintain a specific formation around the moving target. A prescribed performance control scheme is developed to guarantee that relative state trajectories remain within user-defined performance bounds throughout the task. The closed loop system under the proposed control scheme is analytically proven to achieve practical multi-cluster consensus and satisfaction of user-defined performance bounds without requiring knowledge of system parameters. The proposed framework supports various consensus scenarios, including consensus, bipartite consensus, and multi-cluster consensus, offering flexibility in adjusting both the number of clusters and the number of agents in each cluster. We provide numerical simulations to validate the theoretical results.

KEYWORDS

Nonlinear Control, Prescribed Performance Control, Uncertain Systems, Robust Control

1 | INTRODUCTION

In recent years, the study of multi-agent systems in robotics has gained significant attention due to their advantages over single-robot systems ([1] and references therein). Early research in multi-agent systems focused on achieving consensus, where agent states converge to a common value. However, in many robotic applications, multiple robot clusters must function as distinct teams, collaborating on complex tasks with various sub-tasks. Unlike standard linear consensus, where a lack of connectivity can lead to multiple clusters, coordinated team operation requires connectivity and information exchange. Furthermore, connectivity among multiple teams becomes essential when only a subset of agents knows the overall task. In such cases, matrix weights can naturally facilitate multi-cluster consensus. Researchers have studied bipartite consensus in structurally balanced and unbalanced matrix-weighted networks[2,3]. Recent studies have reported distributed control schemes leveraging matrix-weighted interactions to achieve multi-cluster consensus for systems with single-integrator dynamics[4] and double-integrator dynamics[5]. So also, the matrix-scaled consensus for multi-cluster consensus in second-order[6] has been investigated. However, the matrix-weighted multi-cluster consensus problem for agents with more complex nonlinear dynamics remains largely unexplored.

Ensuring the system response satisfies defined performance boundaries is essential for practical applications. Prescribed performance control has emerged to guarantee that errors between communicating agents evolve within predefined bounds.

Notable contributions in this field include bounding the response time and overshoot values for first-order linear systems [7], second-order linear systems [8], controlled evolution of stochastic multiple agents [9] and nonlinear agents [10] with prescribed performance constraints, prescribed performance control based on transient response for multi-input multi-output nonlinear systems [11], prescribed transient, steady-state [12] and fault tolerant [13] performance for uncertain nonlinear system and prescribed performance control based on distance-based formation control for a system with external disturbance [14]. Researchers have designed low-complexity controllers to improve stability and performance for high-order nonlinear multi-agent systems with a directed graph [15] and unknown dynamics [16,17]. A consensus with leader-follower multi-agent systems under prescribed performance conditions has also been studied [18,19]. Formation control of agents with Euler-Lagrangian (EL) dynamics under communication, feasibility, and performance constraints has also been studied [20].

Motivated by the above discussion, this paper addresses the challenge of coordinating multiple robot groups to escort or capture a moving target and form distinct clusters around it. The robot teams act as separate clusters, communicating via a matrix-weighted graph. The robots are modeled as EL systems, making our model applicable to a broad class of robots. We assume all agents have access to the target's trajectory information.

The main contributions of the paper can be highlighted as follows:

1. **Matrix-Weighted Control for Cooperative Target Capture.** A robust matrix-weighted control scheme is developed for the cooperative capture of a target using n EL agents with disturbance. Under sufficient conditions of connectivity and structural balance, the proposed control law u ensures that the agents achieve multi-cluster consensus, forming different clusters around a mobile target at position x_d. This approach is referred to as multi-cluster control.
2. **Flexibility of Cluster Formations.** The paper demonstrates that adjusting a single parameter within the multi-cluster control framework can effectively achieve various cluster configurations, allowing flexible team formations.
3. **Prescribed Performance Control.** A prescribed performance control scheme is introduced to maintain the relative state trajectories within user-defined performance bounds. The objective is to design a control law u such that, in addition to achieving multi-cluster control, guarantees that the edge states remain within the bounds defined by the user. This control law applies to both cyclic and acyclic graphs.
4. **Handling Unknown System Parameters.** Finally, the prescribed performance control guarantees practical multi-cluster consensus, even when the system parameters are unknown.

Organization: The paper is organized as follows. Section 2 provides the overview of the graph's structure. In section 3, we discuss the agent model and the control strategy for achieving multi-cluster consensus. Section 4 outlines the framework for the agents to achieve multi-cluster consensus with prescribed performance. The analytical results are demonstrated in Section 6 by numerical simulations. Section 7 discusses the conclusion and future scope of the work.

2 | PRELIMINARIES

This section discusses the related notations and preliminaries used in the study. We mainly focus on the underlying graph topology and the performance constraints imposed on the system.

2.1 | The Graph

We consider a set of n agents, each of dimension d, interacting over a matrix-weighted graph $\mathcal{G} = (\mathcal{N}, \mathcal{E})$, where $\mathcal{N} = \{1, \ldots, n\}$ is the set of nodes and $\mathcal{E} \subseteq \mathcal{N} \times \mathcal{N}$ is the set of edges interconnecting the nodes. The edges of the graph $\mathcal{G}$ are denoted as $e_1, \ldots, e_m$, where m is the number of edges. The nodes in $\mathcal{G}$ are partitioned into p disjoint subsets $\mathcal{S}_1, \mathcal{S}_2, \ldots, \mathcal{S}_p$, where $\mathcal{S}_1 \cup \mathcal{S}_2 \cup \ldots \cup \mathcal{S}_p = \mathcal{N}$. The weight of an edge from node j to node i is given by the matrix $R_{ij} \in \mathbb{R}^{d \times d}$. If i and j belong to different subsets, R_{ij} is a user-defined matrix; if they belong to the same subset, the matrix weight is the identity matrix I_d. In this paper, we assume the matrix weights to be orthogonal, such that $R_{ij}^{-1} = R_{ij}^{\top}$. Additionally, the graph $\mathcal{G}$ is structurally balanced, which implies that for every closed cycle $\mathcal{C} = (i, j) - (j, k) - \cdots - (l, m) - (m, i)$ in the graph, the product of the matrix weights along the cycle satisfies $R_{ij} R_{jk} \cdots R_{lm} R_{mi} = I_d$. Thus, the graph $\mathcal{G}$ is formulated as a multi-partite, matrix-weighted, and structurally balanced graph [5]. The graph $\mathcal{G}$ can be divided into a matrix-weighted tree graph graph $\mathcal{G}_t$ and another subgraph $\mathcal{G}_c$ such that $\mathcal{G} = \mathcal{G}_t \cup \mathcal{G}_c$.

This framework allows us to define the matrix-weighted incidence matrix as in Definition 1.

Definition 1. [21] (Matrix-weighted Incidence Matrix) A *matrix-weighted incidence matrix*, B, of a matrix-weighted multi-partite graph $\mathcal{G}$ with n nodes and m edges is a block matrix with $n \times m$ blocks, where each block is of dimension $d \times d$. For a bidirectional graph $\mathcal{G}$, the incidence matrix B can be defined by assigning arbitrary directions as,

$$(B)_{ik} = \begin{cases} I_d & \text{if } e_k = (i,j) \in \mathcal{E} \ \& \ i \text{ is the head of the edge } \& \ i,j \in \mathcal{S}_q, q \in \{1,2,\ldots,p\}, \\ -I_d & \text{if } e_k = (j,i) \in \mathcal{E} \ \& \ i \text{ is the tail of the edge } \& \ i,j \in \mathcal{S}_q, q \in \{1,2,\ldots,p\}, \\ -R_{ij} & \text{if } e_k = (j,i) \in \mathcal{E} \ \& \ i \text{ is the tail of the edge } \& \ i \in \mathcal{S}_q \text{ and } j \in \mathcal{S}_r, q,r \in \{1,2,\ldots,p\} \text{ such that } q \neq r, \end{cases} \tag{1}$$

where R_{ij} is the matrix weight of the directed edge from nodes j to i and I_d represents the identity matrix of size d.
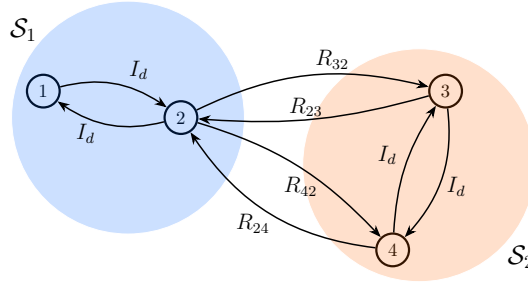

FIGURE 1 Example of a matrix-weighted graph topology. There are four agents partitioned into two clusters. The agents $\{1,2\} \in \mathcal{S}_1$, and the agents $\{3,4\} \in \mathcal{S}_2$.

An example of a matrix-weighted multi-partite graph $\mathcal{G}$ with $n = 4$ agents and $m = 8$ edges is shown in Fig. (1). The agents $\{1,2,3,4\}$ are partitioned into two clusters, $\mathcal{S}_1$ and $\mathcal{S}_2$, where agents $\{1,2\} \in \mathcal{S}_1$ and agents $\{3,4\} \in \mathcal{S}_2$. Each edge in the graph is associated with a matrix weight $R_{ij} \in \mathbb{R}^{d \times d}$. For instance, the edge connecting agent 2 to agent 3 is assigned the matrix weight R_{32}, as agents 2 and 3 belong to different clusters ($\mathcal{S}_1$ and $\mathcal{S}_2$, respectively). Conversely, the edge connecting agents 1 and 2 is assigned the identity matrix I_d, indicating that these agents belong to the same cluster $\mathcal{S}_1$. All edges in Fig. (1) are assigned weights in this manner.

Therefore, using equation (1), we can write the incidence matrix B for Fig. (1) as follows,

$$B = \begin{bmatrix} I_d & -I_d & 0 & 0 & 0 & 0 & 0 & 0 \\ -I_d & I_d & I_d & -R_{12} & I_d & -R_{12} & 0 & 0 \\ 0 & 0 & -R_{21} & I_d & 0 & 0 & -I_d & I_d \\ 0 & 0 & 0 & 0 & -R_{21} & I_d & I_d & -I_d \end{bmatrix}, \tag{2}$$

where the matrix I_d and R_{ij} are of appropriate dimensions. Using the incidence matrix, we now define the Laplacian matrix $\mathcal{L}$ of the graph $\mathcal{G}$ as

$$\mathcal{L} = BB^\top, \tag{3}$$

and the edge Laplacian matrix $\mathcal{L}_e \in \mathbb{R}^{md \times md}$ as

$$\mathcal{L}_e = B^\top B. \tag{4}$$

It is seen that the Laplacian matrix and edge Laplacian matrix are similar to their equivalents in the standard consensus framework [22].

3 | MULTI-CLUSTER CONTROL

This section elaborates on the theory of achieving multi-cluster consensus of multiple agents following Euler-Lagrangian (EL) dynamics.

3.1 | System Dynamics

Defining the position $x = [x_1^\top, \ldots, x_n^\top]^\top \in \mathbb{R}^{nd}$, velocity $v = [v_1^\top, \ldots, v_n^\top]^\top \in \mathbb{R}^{nd}$, control $u = [u_1^\top, \ldots, u_n^\top]^\top \in \mathbb{R}^{nd}$, and the external disturbance $\Delta W = [\Delta w_1, \ldots, \Delta w_n]^\top$, the dynamics of multi-agent system with n agents can be written as,

$$\dot{x} = v,$$
$$\mathbf{M(x)}\dot{v} = -\mathbf{C(x, v)}v - G(x) + u + \Delta W, \tag{5}$$

where $\mathbf{M(x)} = \text{blkdiag}(M_1(x_1), \ldots, M_n(x_n))$, $\mathbf{C(x,v)} = \text{blkdiag}(C_1(x_1, v_1), \ldots, C_n(x_n, v_n))$, $G(x) = [g_1(x_1), \ldots, g_n(x_n)]^\top$ are the symmetric positive definite mass matrix, Coriolis force matrix, and gravitation force matrix, respectively. For our study, we consider n heterogeneous EL agents interacting over a matrix-weighted graph $\mathcal{G}$. We consider the presence of a target in the system, which provides the reference trajectory to the agents, and the reference dynamics is modeled as

$$\dot{x}_d^0 = v_d^0, \tag{6}$$

where x_d^0 and v_d^0 represent the position and velocity of the target, respectively. The derivative of velocity $\dot{v}_d^0$ is assumed to be bounded and continuous over time t. We now define matrix-weighted multi-cluster consensus.

Definition 2. (Matrix-weighted multi-cluster consensus) The multi-agent system is said to reach matrix-weighted cluster multi-consensus around the target's position x_d^0 if the following holds:

- For agents within the same clusters: agents converge to a common value

$$\lim_{t \to \infty} ||(x_i(t) - x_d^0(t)) - (x_j(t) - x_d^0(t))|| = 0,$$

- For agents belonging to distinct clusters: agents converge to states determined by inter-cluster connection weights R_{ij}

$$\lim_{t \to \infty} ||(x_i(t) - x_d^0(t)) - R_{ij}(x_j(t) - x_d^0(t))|| = 0,$$

- Agent velocities converge to v_d,

$$\lim_{t \to \infty} ||(v_i(t) - v_d^0(t))|| = 0.$$

3.2 | Reformulation using Error Variables

For the simplicity of expression, we define position error variable $x_e = x - x_d$ and velocity error variable $v_e = v - v_d$, with $x_d = x_d^0 \otimes \mathbf{1}_n$ and $v_d = v_d^0 \otimes \mathbf{1}_n$, where $\mathbf{1}_n$ is a column vector of size n and entries as 1. Using equation (3), we can write

$$\mathcal{L}(x - x_d) = \mathcal{L}x_e = BB^\top x_e = B\bar{x}, \tag{7}$$

where $\bar{x} = B^\top x_e$. Thus, it can be seen that $\mathcal{L}x_e = 0$ when $\bar{x} = 0$. Multi-cluster consensus, as specified in Definition 2, is satisfied when x_e converges to the null space of the Laplacian matrix $\mathcal{L}$.

3.3 | Control Law for Multi-Cluster Consensus

Let the control u for multi-cluster control be of the form

$$u = -\mathbf{C}\big(-v_d + \mu\mathcal{L}x_e\big) + \mathbf{G} + \mathbf{M}\dot{v}_d - \mu\mathbf{M}\mathcal{L}v_e - k_p\mathcal{L}x_e - K_v\psi_e, \tag{8}$$

where $\psi_e = v_e + \mu\mathcal{L}x_e$, with μ and k_p as positive constants and K_v a symmetric positive definite gain matrix. The stability results are shown in the below theorem.

3.4 | Theorem on Multi-Cluster Consensus

Theorem 1. *Consider a system of n agents, each governed by Euler-Lagrange (EL) dynamics as defined in equation* (5) *and tracking a target trajectory x_d specified in equation* (6). *If the agents are interconnected via a multi-partite, matrix-weighted graph $\mathcal{G}$ that is both connected and structurally balanced, then the feedback control law defined in equation* (8) *ensures that the agents achieve multi-cluster consensus relative to the target trajectory. Specifically, the agents' position error x_e converges asymptotically to the subspace $\{x \in \mathbb{R}^{nd} \mid \mathcal{L}x_e = 0\}$, where:*

$$x_i = x_j, \quad \text{for agents i and j in the same cluster}, \tag{9}$$

$$x_i = R_{ij}x_j, \quad \text{for agents i and j in different clusters}. \tag{10}$$

Proof. Consider the candidate Lyapunov function

$$\mathcal{V}_1 = \frac{1}{2}\psi_e^\top \mathbf{M}\psi_e + \frac{k_p}{2}x_e^\top \mathcal{L}x_e. \tag{11}$$

We can verify that the Lyapunov function $\mathcal{V}_1$ is positive definite. The function $\mathcal{V}_1 = 0$ only when $x_e \in \ker(\mathcal{L})$ and $v = v_d$, i.e., the Lyapunov function is zero only for our desired equilibrium set. Now, calculating the derivative of $\mathcal{V}_1$ with respect to time, we get

$$\dot{\mathcal{V}}_1 = \psi_e^\top \mathbf{M}\dot{\psi}_e + \frac{1}{2}\psi_e^\top \dot{\mathbf{M}}\psi_e + k_p x_e^\top \mathcal{L}\dot{x}_e.$$

Substituting the equation (8), we get

$$\dot{\mathcal{V}}_1 = \psi_e^\top \left(-\mathbf{C}v - \mathbf{C}\left(-v_d + \mu\mathcal{L}x_e\right) - k_p\mathcal{L}x_e - K_v\psi_e + \Delta W\right) + \frac{1}{2}\psi_e^\top \dot{\mathbf{M}}\psi_e + k_p x_e^\top \mathcal{L}v_e.$$

The terms $-\mathbf{C}v - \mathbf{C}(-v_d + \mu\mathcal{L}x_e)$ can be written as $-\mathbf{C}\psi_e$, hence,

$$\dot{\mathcal{V}}_1 = -\psi_e^\top \mathbf{C}\psi_e - k_p\psi_e^\top \mathcal{L}x_e - \psi_e^\top K_v\psi_e + \psi_e^\top \Delta W + \frac{1}{2}\psi_e^\top \dot{\mathbf{M}}\psi_e + k_p x_e^\top \mathcal{L}v_e.$$

We know that for EL systems, $\dot{M} - 2C$ is skew-symmetric[23]. Therefore, on applying this property, $-\psi_e^\top \mathbf{C}\psi_e + \frac{1}{2}\psi_e^\top \dot{\mathbf{M}}\psi_e$ vanishes, and further simplifying, we obtain

$$\dot{\mathcal{V}}_1 = -\psi_e^\top K_v\psi_e - k_p\mu x_e^\top \mathcal{L}\mathcal{L}x_e + \psi_e^\top \Delta W < 0.$$

This proves the asymptotic stability of the system relative to the equilibrium set. Thus, we can infer that x_e converges to the null space of the multi-partite Laplacian matrix $\mathcal{L}$, and the velocity of the agents v_i goes to v_d. □

Theorem 1 establishes that the agent states relative to the target achieve multi-cluster consensus; however, it does not guarantee adherence to the specified performance constraints. The following section addresses the prescribed performance requirements.

4 | PRESCRIBED PERFORMANCE CONTROL

4.1 | Performance Constraints

In real-world applications, system performance is a crucial factor in determining overall effectiveness. Specifically, system states must be constrained to ensure the relative position of agents remains within the user-prescribed performance bounds. For an edge $e_k = (j, i) \in \mathcal{E}$, the evolution of the relative position of agents i and j can be written as

$$\bar{x}_k = (x_i - x_d^0) - R_{ij}(x_j - x_d^0). \tag{12}$$

Similarly, all $\bar{x}$ can be collectively expressed as a single column vector, $\bar{x} = [\bar{x}_1^\top, \ldots, \bar{x}_m^\top]^\top \in \mathbb{R}^{md}$. Let the performance constraint for each element of $\bar{x}$ is gives as:

$$-\rho_{kl}(t) < \bar{x}_{kl}(t) < \rho_{kl}(t), \forall\, t \geq 0, \tag{13}$$

with $l \in \{1, 2, \ldots, d\}$ and the performance limit $\rho_{kl}(t)$ as,

$$\rho_{kl}(t) = (\rho_{kl0} - \rho_{kl\infty})e^{-\epsilon_{kl}t} + \rho_{kl\infty}, \tag{14}$$

where $\rho_{kl0}, \rho_{kl\infty}$ and ϵ_{kl} are positive constants such that $\rho_{kl0} \geq \rho_{kl\infty} > 0$, and $l \in \{1, \ldots, d\}$. The next subsection shows the formulation of the prescribed performance problem in terms of modulated error variables and their transformations.

4.2 | Reformulation in terms of Modulated Error Variables

To ensure that the system meets the performance specifications, we construct a modulated error function,

$$\hat{x}_{kl} = \frac{\bar{x}_{kl}}{\rho_{kl}}. \tag{15}$$

The modulated error is a normalization of the relative position of the agents, $\bar{x}_{kl}$, with respect to the prescribed performance function, ρ_{kl}. It can be seen that, normalized error $\hat{x}_{kl}$ belongs to set,

$$\mathcal{D}_{kl} := \left\{ \hat{x}_{kl}(t) : \hat{x}_{kl}(t) \in (-1, 1) \right\}. \tag{16}$$

which is equivalent to equation (13). The modulated error is transformed using the transformation function $T_{kl}(\hat{x}_{kl})$ as given below:

$$\xi_{kl} = T_{kl}(\hat{x}_{kl}) = \ln\left(\frac{1 + \hat{x}_{kl}}{1 - \hat{x}_{kl}} \right). \tag{17}$$

The performance specifications are met when ξ_{kl} values remain bounded for all the edges. The transformed error dynamics can be obtained by differentiating ξ_{kl} with respect to time t as,

$$\dot{\xi}_{kl} = \phi_{kl}(\hat{x}_{kl}, t)(\dot{\bar{x}}_{kl} + \alpha_{kl}(t)\bar{x}_{kl}), \tag{18}$$

where

$$\phi_{kl}(\hat{x}_{kl}, t) = \frac{2}{(1 - \hat{x}_{kl}^2)} \frac{1}{\rho_{kl}} > 0, \quad \alpha_{kl}(t) = -\frac{\dot{\rho}_{kl}}{\rho_{kl}} > 0. \tag{19}$$

Defining $\xi = [\xi_1^\top, \ldots, \xi_m^\top]^\top$ with $\xi_k = [\xi_{k1}, \ldots, \xi_{kd}]$, $\boldsymbol{\alpha} = \mathrm{blkdiag}(\alpha_1, \ldots, \alpha_m)$ with $\alpha_k = \mathrm{diag}(\alpha_{k1}, \ldots, \alpha_{kd})$ and $\boldsymbol{\Phi} = \mathrm{blkdiag}(\phi_1(\hat{x}_1, t), \ldots, \phi_m(\hat{x}_m, t))$ with $\phi_k(\hat{x}_k, t) = \mathrm{diag}(\phi_{k1}(\hat{x}_{k1}, t), \ldots, \phi_{kd}(\hat{x}_{kd}, t))$, equation (18) can be rewritten in the matrix form as

$$\dot{\xi} = \boldsymbol{\Phi}(\dot{\bar{x}} + \boldsymbol{\alpha}\bar{x}). \tag{20}$$

From equation (17), it can be verified that the condition in equation (13) is achievable by constraining the transformation error ξ. The control ensures that the agents achieve the specified performance in terms of the evolution of their relative positions, as prescribed by the variable ρ.

4.3 | Prescribed Performance Control with Known Dynamics

We propose a control strategy to solve the problem (3) as discussed in Section 1. First, we consider the system parameters $\boldsymbol{M}$ and $\boldsymbol{C}$ to be known to the controller. Accordingly, the control u is proposed as,

$$u = -\mathbf{C}\left(-v_d + \mu\mathcal{L}x_e \right) + \mathbf{G} + \mathbf{M}\dot{v}_d - \mu\mathbf{M}\mathcal{L}v_e - k_p\mathcal{L}x_e - K_v\psi_e - B\boldsymbol{\Phi}\xi. \tag{21}$$

The following theorem demonstrates the stability of the closed-loop system.

Theorem 2. *Given a system consisting of n agents, each following EL dynamics described in equation (5) organized into p clusters, interacting over a matrix-weighted and structurally balanced graph $\mathcal{G}$. Assuming that the initial conditions fall within the specified range of $(-\rho_0, \rho_0)$, the prescribed performance control scheme u proposed in equation (21) guarantees matrix-weighted multi-cluster consensus of the agent states as defined in Definition 2 and the relative agent states adhere to the user-defined performance criteria given by equation (13) for all times $t \geq 0$ if the following condition holds:*

$$-\mu \lambda_{\min}(\mathcal{L}_e^t) + \epsilon_{\max} < 0, \tag{22}$$

where $\mathcal{L}_e^t$ corresponds to the edge Laplacian of the underlying tree matrix-weighted graph $\mathcal{G}_t$ and $\lambda_{\min}()$ indicates the lowest eigenvalue, and $\epsilon_{\max} = \max\limits_{l \in \{1,\ldots,d\}, j \in \{1,\ldots,m\}} \epsilon_{jl}$ is the maximum rate of decay for the prescribed performance functions.

Proof. Consider the candidate Lyapunov function

$$\mathcal{V}_2 = \frac{1}{2}\psi_e^\top \mathbf{M} \psi_e + \frac{k_p}{2} x_e^\top \mathcal{L} x_e + \frac{1}{2} \xi^\top \xi. \tag{23}$$

Differentiating with respect to time, we get

$$\dot{\mathcal{V}}_2 = \psi_e^\top \mathbf{M} \dot{\psi}_e + \frac{1}{2} \psi_e^\top \dot{\boldsymbol{M}} \psi_e + k_p x_e^\top \mathcal{L} \dot{x}_e + \xi^\top \dot{\xi}. \tag{24}$$

Substituting for $\dot{\psi}_e = (\dot{v}_e + \mu\mathcal{L}v_e)$, $\dot{x}_e = v_e$ and $\dot{\xi} = \Phi(\dot{\bar{x}} + \alpha\bar{x})$, where $\mathbf{M}\dot{v}_e = -\mathbf{C}v - \mathbf{G} + u + \Delta W - \mathbf{M}\dot{v}_d$ with u in equation (21), we get

$$\dot{\mathcal{V}}_2 = \psi_e^\top \left(-\mathbf{C}v - \mathbf{G} + u + \Delta W - \mathbf{M}\dot{v}_d + \mu\mathbf{M}\mathcal{L}v_e \right) + \frac{1}{2}\psi_e^\top \dot{\boldsymbol{M}}\psi_e + k_p x_e^\top \mathcal{L}v_e + \xi^\top \Phi(\dot{\bar{x}} + \alpha\bar{x})$$

$$= \psi_e^\top \left(-\mathbf{C}v - \mathbf{C}\left(-v_d + \mu\mathcal{L}x_e\right) - k_p\mathcal{L}x_e - B\Phi\xi - K_v\psi_e + \Delta W \right) + \frac{1}{2}\psi_e^\top \dot{\boldsymbol{M}}\psi_e + k_p x_e^\top \mathcal{L}v_e + \xi^\top \Phi(\dot{\bar{x}} + \alpha\bar{x}).$$

Rewriting $-\mathbf{C}v - \mathbf{C}\left(-v_d + \mu\mathcal{L}x_e\right)$ as $-\mathbf{C}\psi_e$ and applying the property that $\dot{M}(x) - 2C(x,v)$ is skew-symmetric[23], we get

$$\dot{\mathcal{V}}_2 = \psi_e^\top \left(-k_p\mathcal{L}x_e - K_v\psi_e - B\Phi\xi + \Delta W \right) + k_p x_e^\top \mathcal{L}v_e + \xi^\top \Phi(\dot{\bar{x}} + \alpha\bar{x})$$

$$= -\psi_e^\top K_v\psi_e - k_p v_e^\top \mathcal{L}x_e - k_p\mu x_e^\top \mathcal{L}\mathcal{L}x_e + \psi_e^\top \Delta W - v_e^\top B\Phi\xi - \mu x_e^\top \mathcal{L}B\Phi\xi + k_p x_e^\top \mathcal{L}v_e + \xi^\top \Phi\dot{\bar{x}} + \xi^\top \Phi\alpha\bar{x}.$$

Substituting $\dot{\bar{x}} = B^\top v_e$ and further simplifying, we get

$$\dot{\mathcal{V}}_2 = -\psi_e^\top K_v\psi_e - k_p\mu x_e^\top \mathcal{L}\mathcal{L}x_e + \psi_e^\top \Delta W - \mu x_e^\top \mathcal{L}B\Phi\xi + \xi^\top \Phi\alpha\bar{x}.$$

The term $\mu x_e^\top \mathcal{L}B\Phi\xi$ can be rearranged as $\mu\bar{x}^\top \mathcal{L}_e\Phi\xi$. Therefore, $\dot{\mathcal{V}}_2$ can be written as,

$$\dot{\mathcal{V}}_2 = -\psi_e^\top K_v\psi_e - \mu k_p x_e^\top \mathcal{L}\mathcal{L}x_e + \psi_e^\top \Delta W + \bar{x}^\top (-\mu\mathcal{L}_e + \alpha I)\Phi\xi. \tag{25}$$

From equation (19), it can be seen that Φ is a diagonal matrix with positive elements. We consider two cases.

Case 1: The graph $\mathcal{G}$ is a tree. In this case, $\mathcal{L}_e = \mathcal{L}_e^t$ is positive definite. Therefore, we can replace $\mathcal{L}_e$ with its smallest eigenvalue and α with $\epsilon_{\max}$, the maximum decay rate of the prescribed performance functions.

$$\dot{\mathcal{V}}_2 \leq -\psi_e^\top K_v\psi_e - \mu k_p x_e^\top \mathcal{L}\mathcal{L}x_e + \psi_e^\top \Delta W + \bar{x}^\top (-\mu\lambda_{\min}(\mathcal{L}_e^t) + \epsilon_{\max}I)\Phi\xi. \tag{26}$$

Since μ satisfies equation (22), we have $\dot{\mathcal{V}}_2 < 0$.

Case 2: The graph $\mathcal{G}$ is not a tree and is connected. Then, the graph $\mathcal{G}$ can be partitioned into a union of matrix-weighted tree subgraph $\mathcal{G}_t$ and another subgraph $\mathcal{G}_c$ that consists of all remaining edges, i.e., $\mathcal{G} = \mathcal{G}_t \cup \mathcal{G}_c$. Without loss of generality, let the edges be ordered in such a way that the incidence matrix of the general graph is given by $B = [B_t \ B_c]$, where B_t, B_c are the incidence matrices of the underlying tree subgraph $\mathcal{G}_t$ and the subgraph $\mathcal{G}_c$ respectively. Due to structural balance, the edges corresponding to subgraph $\mathcal{G}_c$ denoted by $\bar{x}_c$ can be written as a linear combination of edges of $\mathcal{G}_t$ denoted by $\bar{x}_t$, i.e., $\bar{x}_c = T^\top \bar{x}_t$, where T is a constant matrix.

As a result, we have

$$B = \begin{bmatrix} B_t & B_t T \end{bmatrix}. \tag{27}$$

Substituting equation (27) and calculating the edge laplacian $\mathcal{L}_e$ from the B matrix in the term $\bar{x}^\top(-\mu\mathcal{L}_e + \alpha I)\Phi\xi$, we get

$$
\begin{aligned}
\bar{x}^\top(-\mu\mathcal{L}_e + \alpha I)\Phi\xi &= \begin{bmatrix} \bar{x}_t \\ \bar{x}_c \end{bmatrix}^\top \left(-\mu \begin{bmatrix} \mathcal{L}_e^t & \mathcal{L}_e^t T \\ T^\top\mathcal{L}_e^t & T^\top\mathcal{L}_e^t T \end{bmatrix} + \alpha I \right) \Phi \begin{bmatrix} \xi_t \\ \xi_c \end{bmatrix} \\
&= -\mu\bar{x}_t^\top \mathcal{L}_e^t \Phi_t \xi_t - \mu\bar{x}_t^\top \mathcal{L}_e^t T \Phi_c \xi_c - \mu\bar{x}_c^\top T^\top \mathcal{L}_e^t \Phi_t \xi_t - \mu\bar{x}_c^\top T^\top \mathcal{L}_e^t T \Phi_c \xi_c + \bar{x}_t^\top \alpha\Phi_t \xi_t + \bar{x}_c^\top \alpha\Phi_c \xi_c,
\end{aligned}
$$

where $\bar{x}_c = T^\top \bar{x}_t$. Now, the term $-\mu\bar{x}_c^\top T^\top \mathcal{L}_e^t \Phi_t \xi_t$ can be rewritten as

$$-\mu\bar{x}_c^\top T^\top \mathcal{L}_e^t \Phi_t \xi_t = -\mu\bar{x}_t^\top TT^\top \mathcal{L}_e^t \Phi_t \xi_t \le -\mu\lambda_{\min}(TT^\top\mathcal{L}_e^t)\bar{x}_t^\top \Phi_t \xi_t \le 0.$$

Similarly,

$$-\mu\bar{x}_t^\top \mathcal{L}_e^t T \Phi_c \xi_c \le -\mu\bar{x}_c^\top \mathcal{L}_e^t \Phi_c \xi_c \le -\mu\lambda_{\min}(\mathcal{L}_e^t)\bar{x}_c^\top \Phi_c \xi_c \le 0.$$

After replacing these terms in $\dot{\mathcal{V}}_2$, we get

$$\dot{\mathcal{V}}_2 \le -\psi_e^\top K_v \psi_e - \mu k_p x_e^\top \mathcal{L}\mathcal{L}x_e + \bar{x}_t^\top\left(\epsilon_{\max} - \mu\lambda_{\min}(\mathcal{L}_e^t)\right)\Phi_t\xi_t + \bar{x}_c^\top\left(\epsilon_{\max} - \mu\lambda_{\min}(\mathcal{L}_e^t)\right)\Phi_c\xi_c. \tag{28}$$

We observe that the first and second terms on the right-hand side of inequality (28) are negative definite. From Eq.(15) and Eq. (17), it follows that ξ is a function of $\bar{x}$. When inequality (22) holds, the function $\dot{\mathcal{V}}_2$ is negative definite. This proves that the agents achieve multi-cluster consensus while satisfying the performance constraints. Thus, we can ensure the asymptotic convergence of the system by appropriately choosing ϵ and μ.

<div align="right">□</div>

Implementing equation (21) requires precise knowledge of system parameters. Prescribed performance control, however, ensures that system errors converge within a user-defined limit without needing exact parameter knowledge. The following subsection provides further details on this.

5 | PRACTICAL MULTI-CLUSTER CONSENSUS CONTROL

In this section, we propose an approach to deal with multi-cluster consensus in multi-agent systems with unknown dynamics. To deal with this, we first define the notion of practical multi-cluster consensus.

Definition 3. (Practical multi-cluster consensus) The multi-agent system achieves practical multi-cluster consensus around the vicinity of the target position x_d^0 if the following holds:

- For agents in the same clusters: agents converge to a neighborhood of the desired convergence point

$$\lim_{t\to\infty}||(x_i - x_d^0) - (x_j - x_d^0)|| \le \sigma,$$

- For agents belonging to distinct clusters: agents converge to states determined by inter-cluster connection weights R_{ij}

$$\lim_{t\to\infty}||(x_i - x_d^0) - R_{ij}(x_j - x_d^0)|| \le \sigma,$$

where σ slightly greater than 0 is the convergence bound, i.e., the maximum error within which the agents converge to the neighborhood of the desired convergence point.

We propose a control strategy that provides the desired system performance, even when the system exhibits unknown dynamics. The control can be defined as

$$u = G - k_p\mathcal{L}x_e - K_v\psi_e - B\Phi\xi \tag{29}$$

Theorem 3. *Consider the graph $\mathcal{G}$, which is matrix-weighted, multi-partitioned, and structurally balanced, having the agents with EL dynamics with unknown parameters as described in equation (5) tracking the target. If the initial conditions of the agents are within the specified range of $(-\rho_0, \rho_0)$, and uncertainties and disturbance are satisfied,*

$$\|\Delta W\| + \|\Gamma\|_{\max} \leq \lambda_{min}(K_v) \|\psi_e\|, \tag{30}$$

these terms are explained in the proof. Then, the control u in equation (29) ensures tracking of the target, guaranteeing practical prescribed performance conditions as defined in Definition 3.

Proof. Considering the same candidate Lyapunov function as in equation (23),

$$\mathcal{V}_3 = \frac{1}{2}\psi_e^\top \boldsymbol{M}\psi_e + \frac{k_p}{2}x_e^\top \mathcal{L}x_e + \frac{1}{2}\xi^\top \xi. \tag{31}$$

Differentiating with respect to time,

$$\dot{\mathcal{V}}_3 = \psi_e^\top \boldsymbol{M}\dot{\psi}_e + \frac{1}{2}\psi_e^\top \dot{\boldsymbol{M}}\psi_e + k_p x_e^\top \mathcal{L}\dot{x}_e + \xi^\top \dot{\xi}. \tag{32}$$

Substituting for $\dot{\psi}_e = (\dot{v}_e + \mu\mathcal{L}v_e)$, $\dot{x}_e = v_e$ and $\dot{\xi} = \Phi(\dot{\bar{x}} + \alpha\bar{x})$, we get,

$$\dot{\mathcal{V}}_3 = \psi_e^\top \boldsymbol{M}(\dot{v}_e + \mu\mathcal{L}v_e) + \frac{1}{2}\psi_e^\top \dot{\boldsymbol{M}}\psi_e + k_p x_e^\top \mathcal{L}v_e + \xi^\top \Phi(\dot{\bar{x}} + \alpha\bar{x}). \tag{33}$$

Having $\boldsymbol{M}\dot{v}_e = -\boldsymbol{C}v - \boldsymbol{G} + u + \Delta W - \boldsymbol{M}\dot{v}_d$ with $u = \boldsymbol{G} - k_p\mathcal{L}x_e - K_v\psi_e - B\Phi\xi$ as in equation (29), we get,

$$\dot{\mathcal{V}}_3 = \psi_e^\top(-\boldsymbol{C}v - \boldsymbol{G} + \boldsymbol{G} - k_p\mathcal{L}x_e - K_v\psi_e - B\Phi\xi + \Delta W - \boldsymbol{M}\dot{v}_d + \mu\boldsymbol{M}\mathcal{L}v_e) + \frac{1}{2}\psi_e^\top \dot{\boldsymbol{M}}\psi_e + k_p x_e^\top \mathcal{L}v_e + \xi^\top \Phi(\dot{\bar{x}} + \alpha\bar{x}). \tag{34}$$

Further rearranging and solving, we get,

$$
\begin{aligned}
\dot{\mathcal{V}}_3 &= -\psi_e^\top \boldsymbol{C}v - \psi_e^\top K_v\psi_e + \psi_e^\top \Delta W - k_p\bar{x}^\top \mathcal{L}_e\bar{x} - \psi_e^\top \boldsymbol{M}\dot{v}_d + \mu\psi_e^\top \boldsymbol{M}\mathcal{L}v_e + \frac{1}{2}\psi_e^\top \dot{\boldsymbol{M}}\psi_e + \bar{x}^\top(-\mu\mathcal{L}_e + \alpha I)\Phi\xi \\
&= -\psi_e^\top K_v\psi_e - k_p\bar{x}^\top \mathcal{L}_e\bar{x} - \psi_e^\top \boldsymbol{C}v - \psi_e^\top \boldsymbol{M}\dot{v}_d + \psi_e^\top \Delta W + \mu\psi_e^\top \boldsymbol{M}\mathcal{L}v_e + \frac{1}{2}\psi_e^\top \dot{\boldsymbol{M}}\psi_e + \bar{x}^\top(-\mu\mathcal{L}_e + \alpha I)\Phi\xi \\
&\leq -\psi_e^\top K_v\psi_e - k_p\bar{x}^\top \mathcal{L}_e\bar{x} + \|\psi_e\|_{\max} \|\Gamma\|_{\max} + \|\psi_e\|_{\max} \|\Delta W\| + \bar{x}^\top(-\mu\mathcal{L}_e + \alpha I)\Phi\xi,
\end{aligned}
\tag{35}
$$

where $\Gamma = \boldsymbol{C}v + \boldsymbol{M}\dot{v}_d - \mu\boldsymbol{M}\mathcal{L}v_e - \dot{\boldsymbol{M}}\psi_e$. Satisfying the inequality in equation (22) results in the last term on the right-hand side of inequality (35) being strictly negative definite. If the disturbance ΔW and uncertain parameters are bounded as,

$$\|\Delta W\| + \|\Gamma\|_{\max} \leq \lambda_{min}(K_v) \|\psi_e\|. \tag{36}$$

Then, $\dot{\mathcal{V}}_3 \leq 0$ proves the system dynamics stable and guarantees adherence to performance conditions.

Note that such a bound is very conservative. Additionally, various terms in the Γ, such as $\boldsymbol{M}$ and $\boldsymbol{C}$, are bounded for any EL system. Control gains K_v, k_p, and μ can be appropriately chosen to ensure the agents can track the desired target satisfying the prescribed performance criteria, even when the system parameters are unknown.

$\square$

6 | SIMULATION RESULTS

In this section, we use numerical simulations to validate the theoretical results. Consider the matrix-weighted graph $\mathcal{G}$, which operates on a 2-D plane of $n = 12$ EL agents and $m = 13$ edges. The illustration of the structure is shown in Fig. (2). The network comprises a set of heterogeneous EL agents with dynamics as discussed in equation (5) with the disturbance as a varying additive disturbance. The parameter M_i of agents $\{1, 2, 3, 4\}$ are given by $M_i = 0.7I_{2\times2}$, agents $\{5, 6, 7, 8\}$ by $M_i = 0.6I_{2\times2}$ and agents $\{9, 10, 11, 12\}$ by $M_i = 0.8I_{2\times2}$ and the parameters C_i and g_i, $i \in \{1, \ldots, 12\}$ of all EL agents are chosen as $C_i = [0\ 0.5; -0.5\ 0]$, $g_i = [9.8, 9.8]^\top$. The matrix $R(\theta)$ represents the interaction between the clusters. For the simulations, we choose this orthogonal
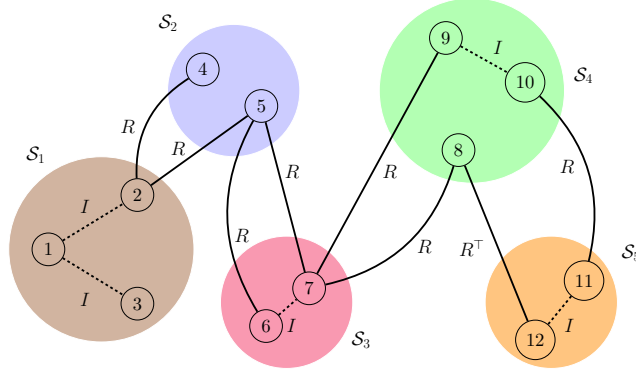
FIGURE 2 The matrix-weighted graph $\mathcal{G}$ with $n = 12$ nodes and $m = 13$ edges, used for numerical simulations. The nodes belong to $p = 5$ clusters, viz, $\{1, 2, 3\} \in S_1$, $\{4, 5\} \in S_2$, $\{6, 7\} \in S_3$, $\{8, 9, 10\} \in S_4$ and $\{11, 12\} \in S_5$.

matrix weight as the 2×2 rotational matrix given by

$$R(\theta) = \begin{bmatrix} \cos\theta & -\sin\theta \\ \sin\theta & \cos\theta \end{bmatrix}, \tag{37}$$

where θ can be chosen for the desired formation. We start the numerical simulations from random initial conditions in the range of $x_i \in [-10, 10]^2$ for both position and velocity. Throughout the figures, the dashed lines show the target trajectory, and the colored lines represent the agent trajectories. The target follows a circular trajectory given by

$$x_d = \begin{bmatrix} 10\cos(0.5t) - 10 & 10\sin(0.5t) \end{bmatrix}^\top. \tag{38}$$

The initial values of $\bar{x}$ are selected such that $-\rho(0) < \bar{x}(0) < \rho(0)$, as specified by equation (14). In this simulation, we choose
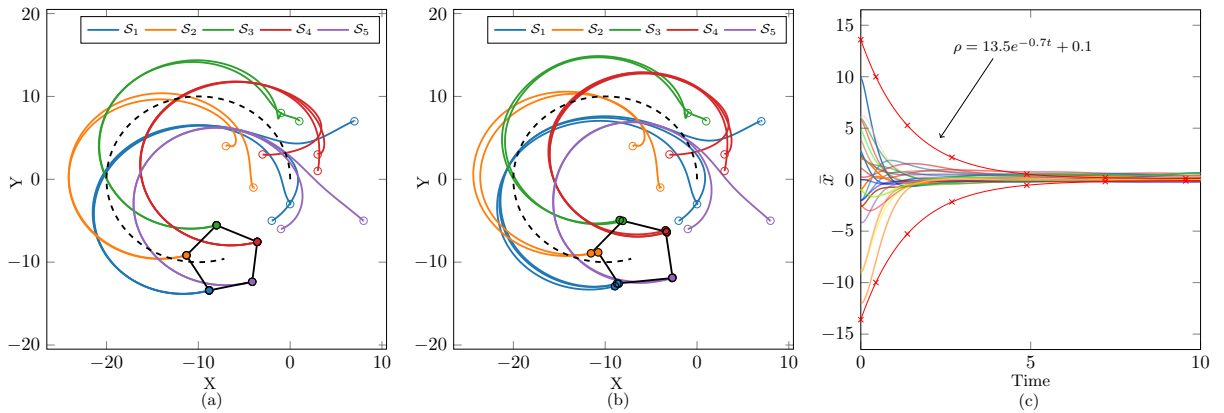

FIGURE 3 Simulation of 12 agents interacting over the graph $\mathcal{G}$ achieving multi-cluster consensus of $p = 5$ clusters. (a) 2D plot of the agents following the target; (b) 2D plot when the system has an external disturbance; (c) Time series plot of $\bar{x}$ when the decay rate is $\epsilon = 0.7$.

$\rho_0 - \rho_\infty = 13.5$, $\rho_\infty = 0.1$ and $\epsilon = 0.7$ for all agents.

We choose $\theta = 2\pi/5$ in equation (37), such that the resultant formation is a pentagon. Fig. (3) (a) shows the trajectories of the 12 EL agents, starting from random positions. Here, it is assumed that the system is disturbance-free. On applying the control u in equation (8), the agents converge to a multi-cluster consensus state of five clusters, each positioned at a vertex of the pentagon.
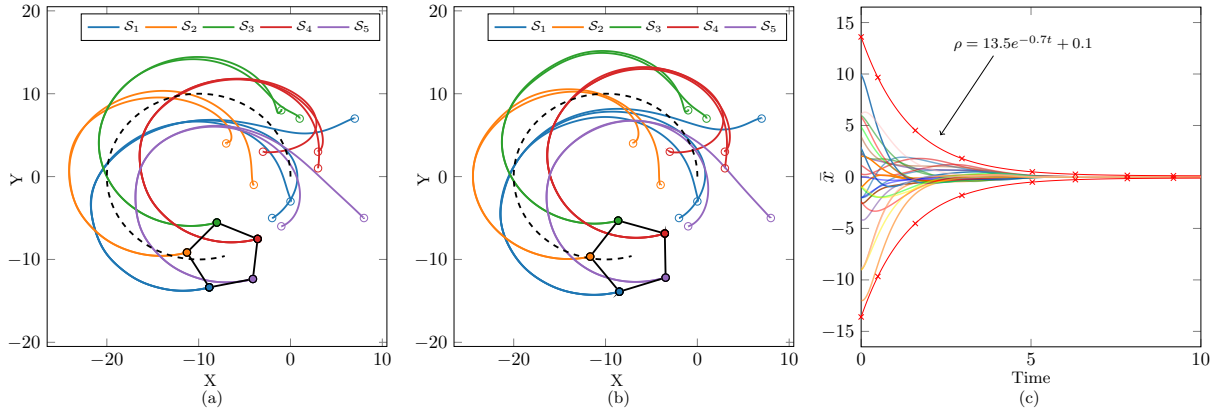
FIGURE 4 Simulation of 12 agents achieving multi-cluster consensus of $p = 5$ clusters adhering to prescribed performance. (a) 2D plot of agents following the target trajectory for a disturbance-free system; (b) 2D plot of the agents when the system has an external disturbance; (c) Time series plot of $\bar{x}$ when decay rate is $\epsilon = 0.7$.

Now, on adding a disturbance to the system, the agents still achieve multi-cluster consensus, forming five clusters as seen in Fig. (3) (b). Fig. (3) (c) shows a time series plot of the relative positions of agents, $\bar{x}$. We see that $\bar{x}$ states are not confined within the user-defined limit ρ, emphasizing the need for a prescribed performance control law.

On applying the prescribed performance control law in equation (21) to the above-discussed system under a disturbance-free system, we see that the agents converge to form the pentagon as seen in Fig. (4) (a). Despite adding an external disturbance, the agents still achieve multi-cluster consensus, as shown in Fig. (4) (b) while adhering to the prescribed limit ρ as demonstrated in Fig. (4) (c). Based on Fig. (4) (c), we can validate that $\bar{x}$, the error in tracking the target, is within the limit ρ prescribed by the user.
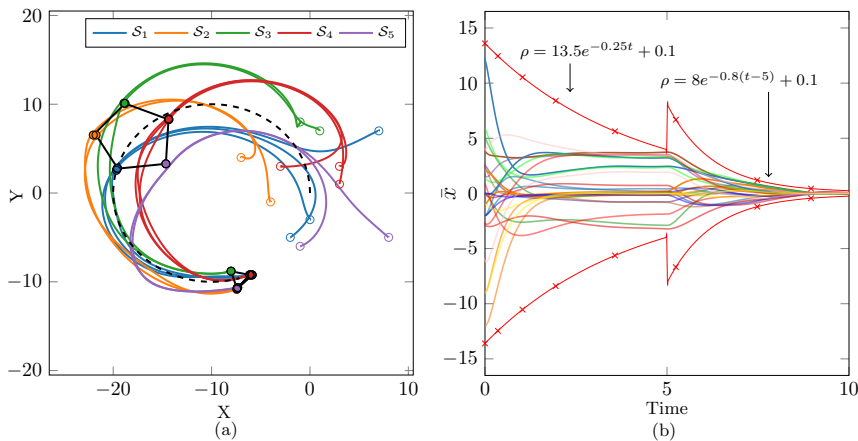

FIGURE 5 Simulation of 12 agents transitioning from $p = 5$ clusters to $p = 3$, while tracking the moving target. (a) The 2D plot of the agents which initially approach a pentagon-shaped five-cluster formation, transitioning later into three clusters when θ is changed; (b) Time series plot of $\bar{x}$ with two different ρ functions

Now, we illustrate that the number of clusters can be adjusted by changing θ. We use the same graph from Fig. (2). The initial conditions and parameters remain the same as mentioned above. Initially, we set $\theta = 2\pi/5$ and then switch to $\theta = 2\pi/3$ at $t = 5$ seconds. The 2D plot from this simulation is shown in Fig. (5)(a). Agents start from random positions, and on applying the control in equation (21), agents approach a state of multi-cluster consensus with five clusters forming a pentagon around the target. At $t = 5$, when θ is changed to $2\pi/3$, the agents adjust positions, transitioning from five clusters to three, effectively tracking the

moving target while maintaining the multi-cluster formation. Fig. (5) (b) shows the time series of $\bar{x}$ as the agents dynamically adjust cluster formations while tracking the target. Initially, edges are bounded by the constraints $\rho = 13.5e^{-0.25t} + 0.1$, switching around $t = 5$ seconds to $\rho = 8e^{-0.8(t-5)} + 0.1$.

We also validate the feasibility of the control in equation (29). As shown in Fig. (6), our multi-cluster consensus scheme remains effective, even when the system dynamics are unknown to the controller. Therefore, we have demonstrated that our
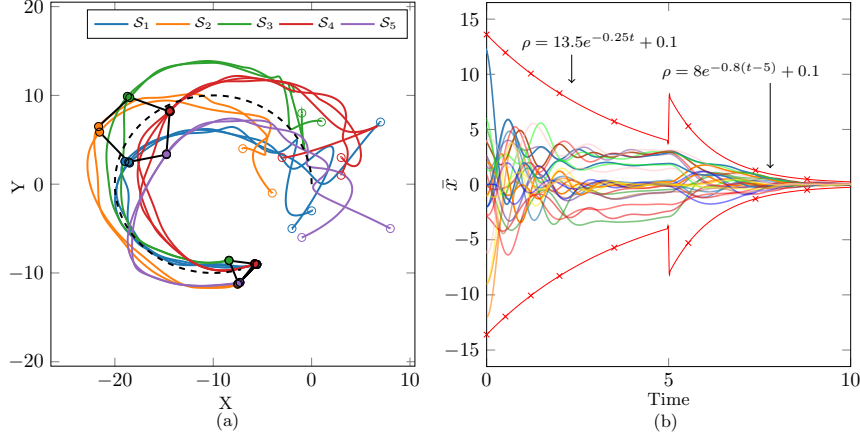

FIGURE 6 Simulation of 12 agents under an external disturbance transitioning from $p = 5$ clusters to $p = 3$, while tracking the moving target. (a) The 2D plot of the agents which initially approach a pentagon-shaped five-cluster formation, transitioning later into three clusters when θ is changed; (b) Time series plot of $\bar{x}$ with two different ρ functions

scheme is capable of handling both external disturbances and uncertainties while also allowing for adjustments in the number of clusters by tuning the parameter θ. In all such cases, the performance consistently remains within the prescribed limits.

7 | CONCLUSION

This paper presented a matrix-weighted control scheme for achieving multi-cluster consensus among agents with nonlinear Euler-Lagrangian dynamics while encircling a moving target. The prescribed performance control scheme ensures that the relative state trajectories remain within user-defined performance bounds, even in the presence of external disturbances. Additionally, the control was modified to handle scenarios where the system parameters are unknown while still maintaining the prescribed performance. Our approach demonstrated flexibility in adjusting the number of clusters and accommodating various graph topologies, including tree graphs and graphs with cycles. In this paper, we have considered a scenario where all agents have complete trajectory information of the target. Additionally, the input is currently presumed to be unbounded. Future research will focus on systems with bounded inputs and situations where only a subset of agents has access to the target's trajectory information.

References

1. Cao Y, Yu W, Ren W, Chen G. An overview of recent progress in the study of distributed multi-agent coordination. *IEEE Transactions on Industrial informatics* 2012; 9(1): 427–438.

2. Pan L, Shao H, Mesbahi M, Xi Y, Li D. Bipartite consensus on matrix-valued weighted networks. *IEEE Transactions on Circuits and Systems II: Express Briefs* 2018; 66(8): 1441–1445.

3. Su H, Chen J, Yang Y, Rong Z. The bipartite consensus for multi-agent systems with matrix-weight-based signed network. *IEEE Transactions on Circuits and Systems II: Express Briefs* 2019; 67(10).

4. Gopika R, Resmi V, Warier RR. Cluster consensus in multi-partitioned matrix weighted graphs. *2022 13th Asian Control Conference (ASCC)* 2022: 1184–1189.

5. Gopika R, Resmi V, Warier RR. Cluster Consensus of Multi-agent Systems with Second Order Dynamics Over Matrix-weighted Graphs. *2022 Eighth Indian Control Conference (ICC)* 2022: 1–6.

6. Trinh MH, Van Vu D, Van Tran Q, Ahn HS. Matrix-scaled consensus. *2022 IEEE 61st Conference on Decision and Control (CDC)* 2022: 346–351.

7. Karayiannidis Y, Dimarogonas DV, Kragic D. Multi-agent average consensus control with prescribed performance guarantees. *2012 IEEE 51st IEEE Conference on Decision and Control (CDC)* 2012: 2219–2225.

8. Macellari L, Karayiannidis Y, Dimarogonas DV. Multi-agent second order average consensus with prescribed transient behavior. *IEEE Transactions on Automatic Control* 2016; 62(10): 5282–5288.

9. Jagtap P, Dimarogonas DV. Distributed Consensus of Stochastic Multi-agent Systems with Prescribed Performance Constraints. *2021 60th IEEE Conference on Decision and Control (CDC)* 2021: 1911–1916.

10. Li YY, Li YX. Decentralized asymptotic tracking control for time-varying interconnected nonlinear systems with prescribed performance. *International Journal of Robust and Nonlinear Control* 2024; 34(15): 10315–10330.

11. Bechlioulis CP, Rovithakis GA. Robust adaptive control of feedback linearizable MIMO nonlinear systems with prescribed performance. *IEEE Transactions on Automatic Control* 2008; 53(9): 2090–2099.

12. Bechlioulis CP, Rovithakis GA. Decentralized robust synchronization of unknown high order nonlinear multi-agent systems with prescribed transient and steady state performance. *IEEE Transactions on Automatic Control* 2016; 62(1): 123–134.

13. Hu Y, Yan H, Wang M, Chang Y, Shi K. Practical preset time fault-tolerant control of uncertain Euler–Lagrange systems with input saturation and guaranteed performance. *International Journal of Robust and Nonlinear Control* 2024; 34(5): 3259–3277.

14. Mehdifar F, Bechlioulis CP, Hashemzadeh F, Baradarannia M. Prescribed performance distance-based formation control of multi-agent systems. *Automatica* 2020; 119: 109086.

15. Katsoukis I, Rovithakis GA. A low complexity robust output synchronization protocol with prescribed performance for high-order heterogeneous uncertain MIMO nonlinear multiagent systems. *IEEE Transactions on Automatic Control* 2021; 67(6): 3128–3133.

16. Min X, Baldi S, Yu W, Cao J. Low-complexity control with funnel performance for uncertain nonlinear multi-agent systems. *IEEE Transactions on Automatic Control* 2023.

17. Xie H, Zhang JX, Jing Y, Chen J, Dimirovski GM. Practical prescribed-time tracking control of unknown nonlinear systems: A low-complexity approach. *International Journal of Robust and Nonlinear Control* 2024; 34(16): 11010–11042.

18. Chen F, Dimarogonas DV. Consensus control for leader-follower multi-agent systems under prescribed performance guarantees. *2019 IEEE 58th Conference on Decision and Control (CDC)* 2019: 4785–4790.

19. Xiong SX, Xie XP, Jiang GP. A distributed containment tracking control of the UAV formation with prescribed performance subject to collision avoidance. *International Journal of Robust and Nonlinear Control* 2024; 34(9): 5813–5832.

20. Min X, Baldi S, Yu W. Funnel-based Asymptotic Control of Leader-Follower Nonholonomic Robots Subject to Formation Constraints. *IEEE Transactions on Control of Network Systems* 2023.

21. Gopika R, Jagtap P, Resmi V, Warier RR, Dhongdi SC. Prescribed Performance Control for Multi-Cluster Consensus using Matrix-Weighted Interactions. *IFAC-PapersOnLine* 2024; 57: 321–326.

22. Mesbahi M, Egerstedt M. *Graph theoretic methods in multiagent networks*. Princeton University Press . 2010.

23. Slotine JJE, Li W, others . *Applied nonlinear control*. 199. Prentice hall Englewood Cliffs, NJ . 1991.